

Fighter Evasive Maneuvers Against Proportional Navigation Missile

Fumiaki Imado* and Susumu Miwa†
Mitsubishi Electric Corporation, Tokyo, Japan

A comparative study of several evasive maneuvers of a fighter against a typical proportional navigation missile is conducted. The aircraft may take a sustained maximum g turn, linear acceleration by maximum thrust, or the optimal evasive maneuver. For various initial conditions in relation to relative range, aspect angle, and altitude, the possible evasive regions are calculated and discussed. Some features of evasive maneuvers intended to lockoff a missile are also studied. The results show that each maneuver has its advantageous region; therefore, a pilot should change evasive strategy, depending on missile-aircraft relative geometry and altitude.

Nomenclature

a	= lateral acceleration
a_c	= missile lateral acceleration command signal
C_D, C_L	= drag and lift coefficients, respectively
C_{D0}	= zero-lift drag coefficient
D	= drag
g	= acceleration of gravity
h	= altitude
J	= performance index
k	= induced drag coefficient of aircraft
k_1, k_2	= drag coefficients of missile
L	= lift
m	= mass
M	= Mach number
MD	= terminal miss distance
N_e	= effective navigation constant
r	= slant range between missile and aircraft
s	= reference area
t	= time
t_e	= sustainer burning time
t_{go}	= initial time-to-go
t_f	= interception time
T	= thrust
v	= velocity
v_c	= closing velocity
x, y	= horizontal coordinates
α, α_0	= angle of attack and zero lift angle
θ	= attitude angle
θ_H	= seeker angle from missile axis
ρ	= air density
σ, ϕ, ψ	= line-of-sight, aircraft-bank, and flight-path angles, respectively
τ	= missile time constant
τ_α	= missile turn rate lag
Ω	= terminal condition in Eqs. (20) and (21)
(\cdot)	= time derivative

Subscripts

$0, f$	= initial and terminal values, respectively
m	= missile
\max, \min	= maximum and minimum values, respectively
t	= aircraft (target)

Introduction

MANY studies have been performed on the optimal evasive maneuver of an aircraft against a tactical missile. In most optimal strategies in these studies, an aircraft strives to maximize terminal miss distance.¹⁻⁶ Such a maneuver has been proved to be very effective, but it seems to be difficult for a pilot to implement. In a more practical situation, a pilot may tend to take an easier maneuver such as a sustained maximum g turn or a simple linear acceleration with an afterburner. It is worth studying the features of these maneuvers, in addition to the optimal maneuvers, and discussing their best evasive region. By employing a fairly precise mathematical model, the calculation of optimum maneuvers and simulation studies are conducted, and the results are presented in this paper. Although not mentioned in previous unclassified papers, a possibility of evading a missile is shown in intentional maneuvers to cause a missile seeker lockoff. Some results for this maneuver are also presented.

Mathematical Model

Figure 1 shows the relative geometry of a missile and an aircraft, as well as the aircraft force balance. For simplicity, motions are constrained within a given horizontal plane. The following equations of motion are used for calculation of the optimal control and simulation study.

Aircraft Motion

The aircraft is modeled as a point mass, and the equations of motion in a horizontal plane are

$$\dot{v}_t = (T_t \cos \alpha - D)/m_t \quad (1)$$

$$\dot{\psi}_t = (L + T_t \sin \alpha)/(m_t v_t) \quad (2)$$

$$\dot{x}_t = v_t \cos \psi_t \quad (3)$$

$$\dot{y}_t = v_t \sin \psi_t \quad (4)$$

where

$$L = \frac{1}{2} \rho v_t^2 s_t C_L, \quad C_L = C_{L\alpha} (\alpha - \alpha_0) \quad (5)$$

$$D = \frac{1}{2} \rho v_t^2 s_t C_D, \quad C_D = C_{D0} + k C_L^2 \quad (6)$$

Two constraints are imposed on the value of C_L ,

$$C_L \leq C_{L\max} \quad C_L \leq m_t a_{t\max} / (\frac{1}{2} \rho v_t^2 s_t) \quad (7)$$

Received Oct. 29, 1985; revision received July 17, 1986. Copyright © American Institute of Aeronautics and Astronautics, Inc., 1985. All rights reserved.

*Chief Engineer, Mechanical Systems and Technology Department, Central Research Laboratory. Member AIAA.

†Manager, Information Network Systems Development, Headquarters.

Missile Motion

The missile lateral acceleration is approximated by a first-order lag to a lateral acceleration command. For simplicity, missile mass is assumed constant. (The effect of the missile mass change can be compensated for by a properly designed autopilot.) The control law of the missile is assumed to be constant-gain proportional navigation with signal saturation taken into consideration; thus,

$$\dot{v}_m = 1/m_m (T_m - D_m) \quad (8)$$

$$\dot{a}_m = (a_c - a_m)/\tau \quad (9)$$

$$\dot{\psi}_m = a_m/v_m \quad (10)$$

$$\dot{x}_m = v_m \cos \psi_m \quad (11)$$

$$\dot{y}_m = v_m \sin \psi_m \quad (12)$$

where

$$D_m = k_1 v_m^2 + k_2 (a_m/v_m)^2 \quad (13)$$

$$T_m(t) = \begin{cases} T_m & \text{for } 0 < t \leq t_e \\ 0 & \text{for } t_e < t \end{cases} \quad (14)$$

$$a_c = \begin{cases} N_e v_c \dot{\sigma} & \text{for } |a_c| \leq a_{c \max} \\ a_{c \max} \text{sign}(a_c) & \text{for } |a_c| > a_{c \max} \end{cases} \quad (15)$$

In Eq. (15), N_e is the effective navigation ratio, v_c the closing velocity, and $\dot{\sigma}$ the line-of-sight turning rate given by

$$v_c = -\dot{r} \quad (16)$$

$$\dot{\sigma} = 1/r^2 [(y_t - y_m)(\dot{x}_t - \dot{x}_m) - (\dot{y}_t - \dot{y}_m)(x_t - x_m)] \quad (17)$$

where r is slant range,

$$r = [(x_t - x_m)^2 + (y_t - y_m)^2]^{1/2} \quad (18)$$

Study Conditions

Assuming an actual aerial combat situation, F-4C⁷, and a typical medium-range air-to-air missile, two typical operation

cases are considered in this study. Three-dimensional study may also be possible but very complicated. A two-dimensional constant-altitude study, like earlier papers,^{1,2,4,5} can provide insight into aspects of this problem and perhaps serve as a basis for three-dimensional study. In the case where the aircraft is pursued by multiple missiles, the evasive region is obtained by superposing the results of the simple missile cases. The parameter values used are presented in Table 1.

Sustained Maximum g Turn and Linear Acceleration by Maximum Thrust

The natural behavior of a pilot chased by a missile may be to maneuver his aircraft immediately into a sustained maximum g turn. On the other hand, for current high- T/W -ratio aircraft, shaking off the missile by simply accelerating an aircraft with an afterburner may be very effective. These two types of maneuvers are very easy for the pilot; therefore, they are frequently employed.

The calculated evasive regions for two typical altitudes of 4572 and 10,668 m are shown in Figs. 2 and 3. In these figures, the triangle positioned at the origin denotes an aircraft that turns clockwise with maximum sustained g or moves straight forward at an initial velocity of 0.9 M . Maximum (afterburner) thrust is employed in both cases. The surrounding sets of arrows denote the initial position of missiles and their direction of velocity vectors which lie in collision courses. The missile speed is $M=2$, with 8-s sustainer fuel left. The hatched regions show the successful evasive region by the sustained maximum g turn and linear acceleration by maximum thrust. In the upper half-plane, the evasive region by sustained maximum g turn is divided into two portions, inner and outer, and

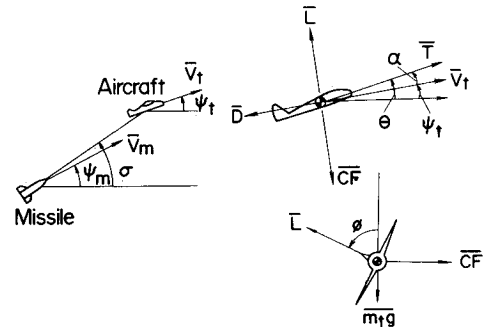


Fig. 1 Relative geometry and aircraft force balance.

Table 1 Parameters	
Aircraft	
m_t	= 17,656 kg
s_t	= 49.24 m ²
Case 1 (Medium altitude: $h = 4572$ m)	
v_{t0}	= 290.2 m/s (0.9 M)
$C_{L\alpha}$	= 3.73/rad
$a_{t \max}$	= 7 g (sustained)
C_{D0}	= 0.0202 $k = 0.198$
T_{\max}	= 219,755 N (afterburner)
Case 2 (High altitude: $h = 10,668$ m)	
v_{t0}	= 266.9 m/s (0.9 M)
$C_{L\alpha}$	= 3.83/rad
$a_{t \max}$	= 2 g (sustained)
C_{D0}	= 0.0293 $k = 0.161$
T_{\max}	= 109,878 N (afterburner)
Missile	
m_m	= 200 kg
T_m	= 6000 N $t_e = 8.0$ s
$a_{c \max}$	= 30 g
τ	= 0.3 s $N_e = 3$
Case 1 ($h = 4572$ m)	
v_{m0}	= 645 m/s (2.0 M)
k_1	= 0.01041 kg/m $k_2 = 1.038 \times 10^5$ kgm
Case 2 ($h = 10,668$ m)	
v_{m0}	= 593 m/s (2.0 M)
k_1	= 0.00513 kg/m $k_2 = 2.11 \times 10^5$ kgm

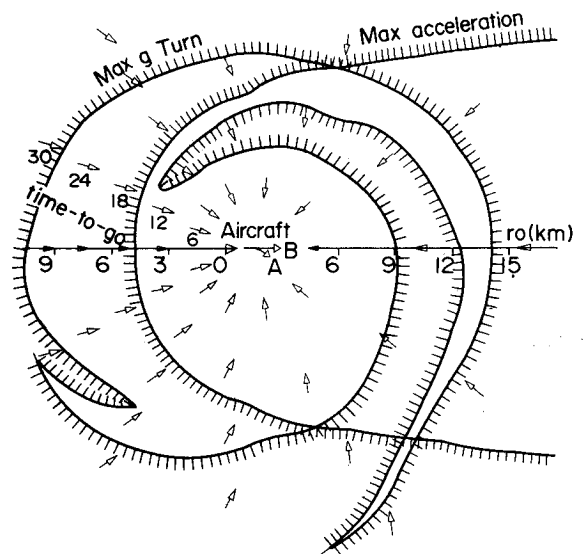


Fig. 2 Evasive region by sustained maximum g turn and linear acceleration by maximum thrust at medium altitude.

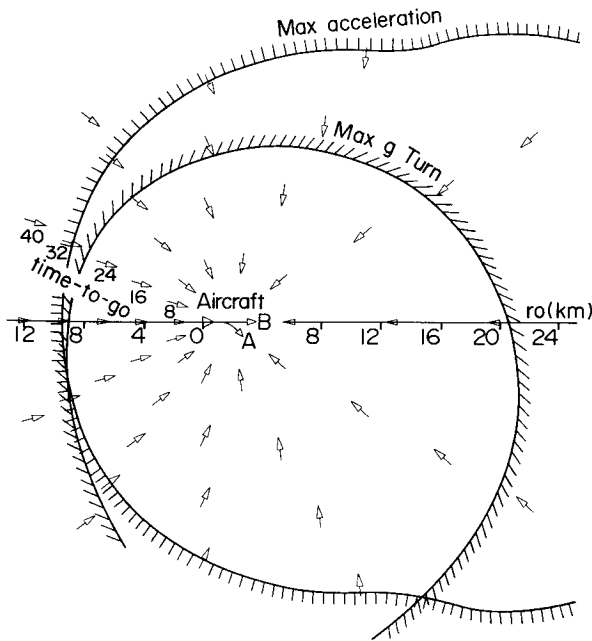


Fig. 3 Evasive region by sustained maximum g turn and linear acceleration by maximum thrust at high altitude.

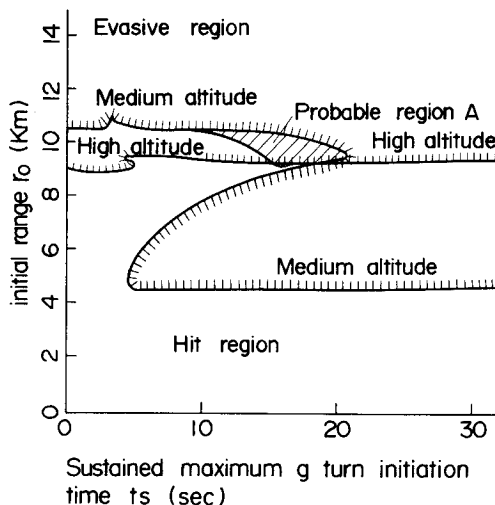


Fig. 4 Evasive region by delayed sustained maximum g turn (tail-chase).

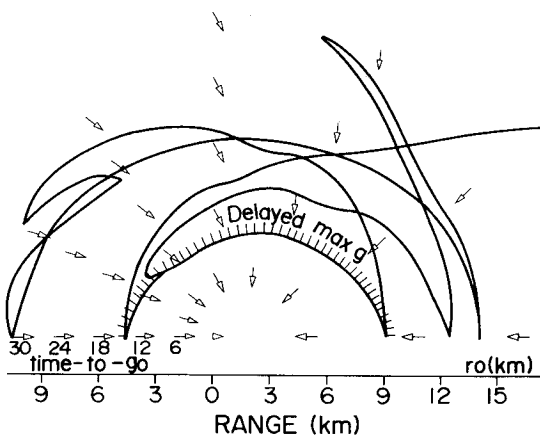


Fig. 5 Evasive region by delayed sustained maximum g turn at medium altitude.

a large gap appears between them. In the inner portion, a missile cannot follow the aircraft turn rate because of lack of navigation time. In the outer portion, a missile cannot follow the aircraft owing to lack of fuel. This gap becomes smaller and gradually diminishes in the lower half-plane. The evasive region by linear acceleration covers mainly the tail-chase region, but it is worthwhile to note that, up to 120-deg initial aspect angle, this maneuver is as effective as the sustained maximum g turn. This is because the sustained maximum g turn loses its effectiveness as the aircraft velocity decreases due to induced drag.

At a higher altitude of 10,668 m (35,000 ft), the performance of an aircraft is greatly degraded, but a missile can still maintain its maximum g performance. As seen in Fig. 3, the missile is effective at far greater distances, and the gap of the low-altitude case diminishes. In actual combat, it is very hard to detect a missile at great distances; thus, it is difficult to evade a missile at high altitude.

Effect of Delayed Sustained g Initiation

In the preceding cases, it is assumed that the sustained maximum g turn starts immediately. A more skilled pilot may delay the maneuver depending on the relative distance. This maneuver may be more difficult to implement than the preceding immediate sustained maximum g turn, but it is far easier than the optimal maneuver presented in the next section.

Figure 4 shows the calculated evasive region at an initial aspect of 0 deg (pure tail chase).

The abscissa is the time t_s when the aircraft initiates the sustained maximum g turn, and the ordinate is the initial relative range r_0 . The successful evasive regions at 4572 and 10,668 m are shown by hatched lines. Because of the highly nonlinear characteristics of the pursuit-evasion problem, the possibility of evasion becomes uncertain in region A.

For example, at $h = 4572$ m and $r_0 = 4.6$ km, a sustained maximum g turn is successful only when a pilot initiates it 5–10 s after initial relative geometry. At $r_0 = 5$ km, a pilot can initiate it anytime after 4.3 s. This means that a pilot can evade even if he does not employ a sustained maximum g turn, which corresponds to the linear acceleration by maximum thrust described in the previous section.

In the medium-altitude case, the delayed sustained maximum g turn extends the evasive region in which an instantaneous turn cannot succeed. Figure 5 shows the coverage by the delayed sustained maximum g turn.

On the other hand, as shown in Fig. 4, the range is not altered by delay time in the high-altitude case. Thus, the successful evasive region cannot be extended by this maneuver.

Optimal Maneuver

Optimal evasive maneuvers are difficult to implement but very effective. Various versions in relation to the criterion for optimality can be considered. The criterion adopted here is that an aircraft maneuvers to maximize the terminal miss. Many studies have been performed on this version, but most of them dealt with it in a very simplified manner, whereas the present study uses a fairly precise model.

Mathematically, this maneuver is obtained by maximizing the terminal criterion function J in regard to aircraft angle of attack α and thrust T ,

$$J = [(x_t - x_m)^2 + (y_t - y_m)^2] t_f \quad (19)$$

under the system equations and constraints (1–18). Terminal time t_f is the time when the next minimum range condition occurs,

$$\Omega \equiv (x_t - x_m)(\dot{x}_t - \dot{x}_m) + (y_t - y_m)(\dot{y}_t - \dot{y}_m) = 0 \quad (20)$$

As is well known, this type of problem is reduced to a nonlinear two-point boundary-value problem, and several

methods have been developed to solve this. In this paper the steepest ascent method^{8,9} is employed.

Our previous study⁶ showed that the optimal evasive maneuver involves turning to be parallel with the missile at first, then steering in the opposite direction with maximum attainable g 's. The resulting maneuver becomes something like a vertical or horizontal S. In Fig. 6, against a missile from the left rear, the optimal maneuver becomes like A, and against a missile from the left front, it becomes like B. The numbered contour lines show the MD resulting from these maneuvers. A complete contour of $MD=10$ m is superimposed over Fig. 2 and shown in Fig. 7. Figure 7 shows that the pilot can have a chance to survive by employing the optimal maneuver in the region where he cannot evade by easier maneuvers.

Figure 8 shows typical histories of aircraft angle of attack α and thrust T (negative α is a positive α with 180-deg roll). The resulting MD depends critically on quick roll timing. Aircraft maximum g performance a_{tmax} and missile time constant τ are also important factors. In practice, this is a last-ditch maneuver when earlier and easier maneuvers do not work.

At an altitude of 10,668 m, this maneuver does not work well due to the decrease in aircraft performance, and the resulting MD hardly exceeds 8 m. This maneuver becomes employable against a missile of $\tau=0.5$ s, and the resulting MD lines of this case are shown in Fig. 9.

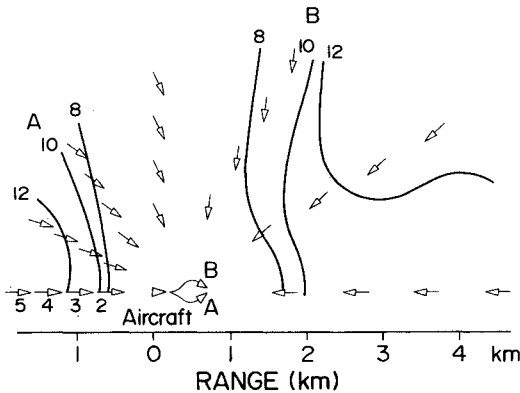


Fig. 6 Evasive region by optimal maneuver at medium altitude with $\tau=0.3$ s.

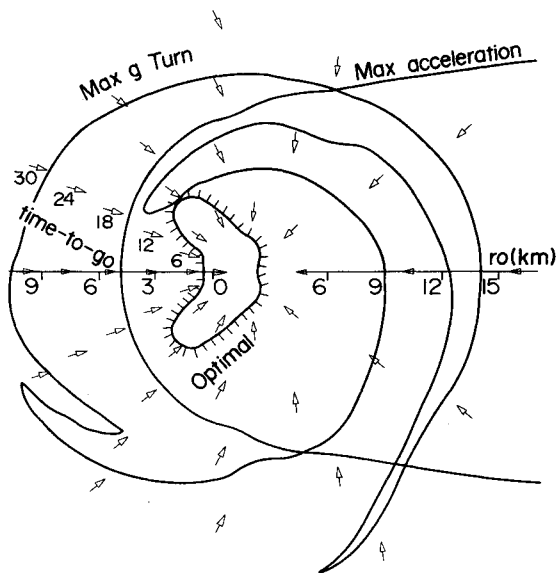


Fig. 7 Evasive region by optimal maneuver, sustained maximum g turn, and linear acceleration at medium altitude.

Maneuver to Cause Missile Lockoff

In the previous section, the limitation of a missile seeker field of view was not taken into consideration. Recent improvements in missile homing heads have made it difficult for an aircraft to evade the missile field of view, but there is still a possibility of evasion under some conditions.

Mathematically, this maneuver is obtained in the same way as the previous problem by maximizing the range by which the aircraft moved outside the seeker field of view. The next ter-

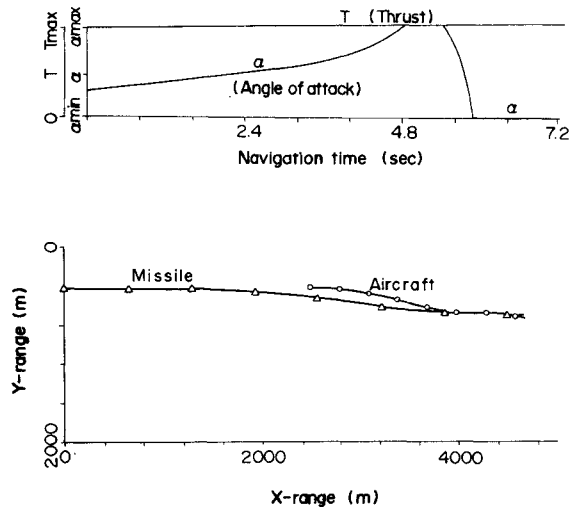


Fig. 8 A typical optimal maneuver trajectory at medium altitude (tail chase).

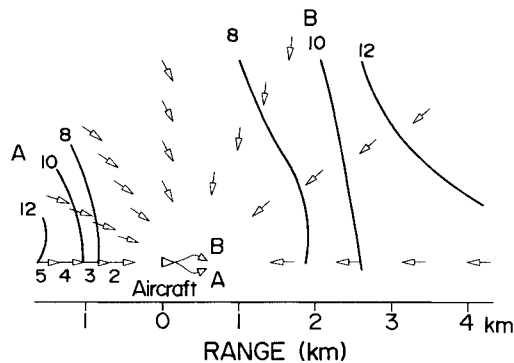


Fig. 9 Evasive region by optimal maneuver at high altitude with $\tau=0.5$ s.

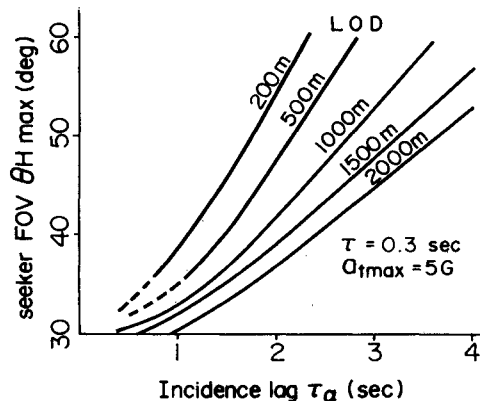


Fig. 10 LOD vs τ_α and θ_{Hmax} (head-on).

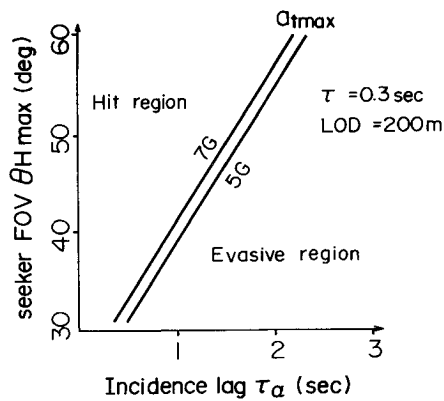


Fig. 11 200-m LOD line vs τ_α and θ_{Hmax} (head-on).

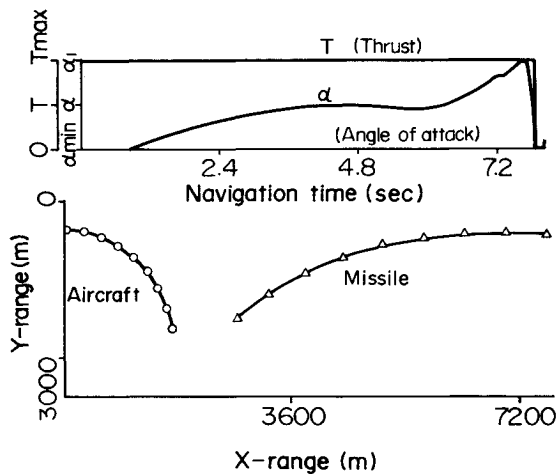


Fig. 12 A typical maneuver trajectory to cause missile lockoff (head-on).

minimal condition is used instead of Eq. (20).

$$\Omega = (\theta_m - \sigma)^2 - \theta_{Hmax}^2 = 0 \quad (21)$$

The missile attitude angle θ_m is approximated by

$$\theta_m = \psi_m + \tau_\alpha / v_m a_m \quad (22)$$

where τ_α denotes the missile incidence lag. Figure 10 shows a calculated example of lockoff distance (LOD), the distance where Eq. (21) occurs, in relation to τ_α and the seeker maximum field of view θ_{Hmax} . Note that since the missile still approaches the aircraft after seeker lockoff occurs, the actual MD becomes far smaller than LOD. Figure 10 shows the 200-m LOD line in relation to aircraft maximum g , a_{tmax} . In Figs. 10 and 11, initial relative range is 7500 m and case 1 data of Table 1 are employed, except for the missile acceleration command a_{cmax} , which is selected as 20 g . From these figures the effects of τ_α and θ_{Hmax} on LOD are large, but the effect of a_{tmax} is small. This is because the maneuver employs intermediate g and not necessarily maximum g . Figure 12 shows an example of trajectory and control history of an aircraft with this maneuver. Figure 13 shows a calculated example of τ_α in relation to velocity and altitude. At high altitude, even though aircraft attainable maximum g degrades, missile τ_α increases as shown in Fig. 13, and with a favorable initial aspect angle, an aircraft may have a chance to survive by this maneuver; however, as it employs an intermediate g , it seems even more difficult to implement than the previously mentioned optimal maneuver.

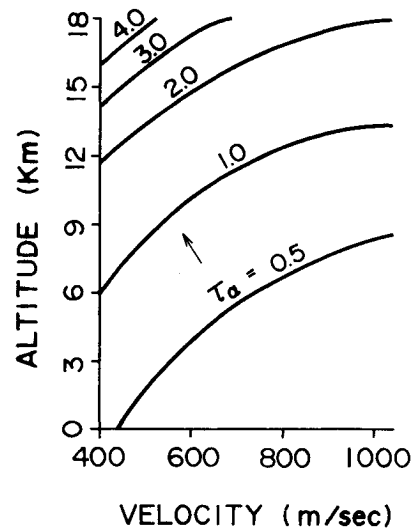


Fig. 13 A calculation example of missile incidence lag in relation to velocity and altitude.

Conclusions

Some features of the results can be summarized as follows.

In the medium altitude of 4572 m, with enough time-to-go for tail-chase or near-tail-chase cases, simple linear acceleration with an afterburner is most efficient. This is the easiest maneuver, and up to the point of 120-deg line-of-sight beam-attack cases, which are head-on rather than tail-chases, it is even more effective than a sustained maximum g turn. With a relatively short time-to-go, there is a region where a sustained maximum g turn is more effective. For near-head-on cases, a sustained maximum g turn should be employed. Whether to take a clockwise or counterclockwise turn depends on the initial aspect angle and relative range.

The sustained maximum g turn effective region is extended by delaying the start of the maneuver. In the region where these easier maneuvers are not successful (very short time-to-go region), only the optimal maneuver is effective and usually gives a pilot a chance to survive. In this maneuver, quick roll timing is a critical factor and many other considerations must be left to chance.

In the high altitude of 10,668 m, the evasive region becomes far distant and the actual difficulty of detecting a missile from far off makes it difficult to evade a missile. Because of degradation of the aircraft maximum attainable g , the optimal maneuver is not effective either. Under some conditions of initial large aspect angle, a narrow seeker field of view, and a relatively large missile incidence lag, a maneuver to cause missile lockoff has a chance to succeed, but it usually employs an intermediate g and may therefore be even more difficult than the optimal maneuver.

Acknowledgments

The authors are indebted to Dr. S. Uehara, Director, Technical Intelligence and Standards Department TRDI of the Japan Defense Agency, for giving us useful advice and discussing the paper. The authors also thank Mr. T. Ishiwara, former fighter pilot and current manager of Mitsubishi Electric Corporation, for his experienced views on air combat tactics.

References

- Julich, P.M. and Borg, D.A., "Proportional Navigation vs an Optimally Evading, Constant Speed Target in Two Dimensions," *Journal of Spacecraft*, Vol. 7, Dec. 1970, pp. 1454-1457.
- Slater, G.L. and Wells, W.R., "Optimal Evasive Tactics Against a

Proportional Navigation Missile with Time Delay," *Journal of Spacecraft*, Vol. 10, May 1973, pp. 309-313.

³Shinar, J., Rotsztein, Y., and Bezner, E., "Analysis of Three-Dimensional Optimal Evasion with Linearized Kinematics," *Journal of Guidance and Control*, Vol. 2, Sept.-Oct. 1979, pp. 353-360.

⁴Forte, I., Steinberg, A., and Shinar, J., "The Effect of Non-Linear Kinematics in Optimal Evasion," *Optimal Control Application & Methods*, Vol. 4, 1983, pp. 139-152.

⁵Anderson, G.M., "Comparison of Optimal Control and Differential Game Intercept Missile Guidance Laws," *Journal of Guidance*

and Control, Vol. 4, March-April 1981, pp. 109-115.

⁶Imado, F. and Miwa, S., "The Optimal Evasive Maneuver of a Fighter Against Proportional Navigation Missiles," AIAA Paper 83-2139, Aug. 1983.

⁷Heffley, R.K. and Jewell, W.F., "Aircraft Handling Qualities Data," NASA CR-2144, Dec. 1972, pp. 61-107.

⁸Bryson A.E. Jr., and Denham, W.F., "A Steepest Ascent Method for Solving Optimum Programming Problems," *Journal of Applied Mechanics*, Vol. 29, June 1962, pp. 247-257.

⁹Bryson A.E. Jr., and Ho, Y.C., *Applied Optimal Control*, Ginn-Blaisdell, Waltham, MA, 1969, pp. 221-228.

From the AIAA Progress in Astronautics and Aeronautics Series . . .

AERO-OPTICAL PHENOMENA—v. 80

Edited by Keith G. Gilbert and Leonard J. Otten, Air Force Weapons Laboratory

This volume is devoted to a systematic examination of the scientific and practical problems that can arise in adapting the new technology of laser beam transmission within the atmosphere to such uses as laser radar, laser beam communications, laser weaponry, and the developing fields of meteorological probing and laser energy transmission, among others. The articles in this book were prepared by specialists in universities, industry, and government laboratories, both military and civilian, and represent an up-to-date survey of the field.

The physical problems encountered in such seemingly straightforward applications of laser beam transmission have turned out to be unusually complex. A high intensity radiation beam traversing the atmosphere causes heat-up and breakdown of the air, changing its optical properties along the path, so that the process becomes a nonsteady interactive one. Should the path of the beam include atmospheric turbulence, the resulting nonsteady degradation obviously would affect its reception adversely. An airborne laser system unavoidably requires the beam to traverse a boundary layer or a wake, with complex consequences. These and other effects are examined theoretically and experimentally in this volume.

In each case, whereas the phenomenon of beam degradation constitutes a difficulty for the engineer, it presents the scientist with a novel experimental opportunity for meteorological or physical research and thus becomes a fruitful nuisance!

Published in 1982, 412 pp., 6 × 9, illus., \$29.50 Mem., \$59.50 List

TO ORDER WRITE: Publications Dept., AIAA, 1633 Broadway, New York, N.Y. 10019